Gene editing of putative cAMP and Ca^{2+}-regulated proteins using an efficient cloning-free CRISPR/Cas9 system in *Trypanosoma cruzi*

Miguel A. Chiurillo[1*], Milad Ahmed[1], César González[1,2], Aqsa Raja[1], and Noelia Lander[1*]

[1]*Department of Biological Sciences, University of Cincinnati, Cincinnati, Ohio 45221-006, United States of America.*

[2]*Escuela e Medicina y Ciencias de la Salud. Instituto Tecnológico y de Estudios Superiores de Monterrey. Monterrey, Nuevo Leon, Mexico.*

***Correspondence**.
M.A. Chiurillo, Department of Biological Sciences, University of Cincinnati, Cincinnati, OH 45221-006, United States of America.
Telephone number: (+1) 513-556-9758
Fax number: (+1) 513-556-5299
e-mail: chiurima@ucmail.uc.edu

N. Lander, Department of Biological Sciences, University of Cincinnati, Cincinnati, OH 45221-006, United States of America.
Telephone number: (+1) 513-556-9798
Fax number: (+1) 513-556-5299
e-mail: landernm@ucmail.uc.edu

Keywords: Calcium ions, Cyclic AMP, Essential genes, Genome editing, Trypanosomes.

ABSTRACT

Trypanosoma cruzi is the causative agent of Chagas disease, a prominent cause of heart disease in the Americas, for which there is no vaccine or satisfactory treatment available. The life cycle of this protozoan parasite alternates between mammalian and insect hosts, during which, in order to survive, it must adapt to a diversity of environmental conditions it faces. The adaptation to these changes is mediated by signaling pathways that coordinate the cellular responses to the new environmental settings. Cyclic AMP (cAMP) and Calcium (Ca^{+2}) signaling pathways regulate critical cellular processes in this parasite, such as differentiation, osmoregulation, flagellar function, host cell invasion and cell

bioenergetics. From the adaptation of CRISPR/Cas9 technology in *T. cruzi* the reverse genetic approaches for functional analysis of genes have experienced a significant impulse However, the toolbox for genome editing in this parasite still needs to be expanded, for example, to perform multiple gene deletion analyses. Here we used a T7RNAP/Cas9-mediated strategy to tag and delete three genes putatively involved in cAMP and Ca^{2+} signaling pathways: a putative Ca^{2+}/calmodulin-dependent protein kinase (*CAMK*), FLAgellar Member 6 (*FLAM6*) and Cyclic nucleotide-binding domain/C2 domain-containing protein (*CC2CP*). We were able to endogenously tag these three genes and determine the subcellular localization of the tagged proteins. Furthermore, the strategy used for gene knockout experiments allows us to suggest that *TcCC2CP* is an essential gene in *T. cruzi* epimastigotes. Our results obtained in *T. cruzi* epimastigote forms on these proteins will open new venues for future research.

INTRODUCTION

Chagas disease is one of the 20 neglected tropical diseases affecting about 1 billion people in the world. This vector-borne infectious disease is caused by the protozoan parasite *Trypanosoma cruzi* and affects 6 to 7 million people in 21 Latin American countries, where the disease is endemic. This infection is considered a leading cause of disability and premature death in the Americas, although most affected individuals remain undiagnosed and untreated (WHO, 2020). There is no vaccine to prevent Chagas disease or satisfactory treatment for chronic patients. If untreated, the infection persists for a lifetime, causing chronic cardiomyopathy or dilatation of the gastrointestinal tract in one-third of the infected population, several years or even decades after the initial contagion (Bonney et al., 2019). Understanding *T. cruzi* biology is crucial to develop alternative strategies to diagnose and treat this silent disease.

Developmental transformations involve key physiological processes for parasite survival. *T. cruzi* has a complex life cycle involving four main developmental stages that colonize very specific niches within its hosts, transitioning between stages in response to microenvironmental changes (Lander et al., 2021; Melo et al., 2020). The signal transduction pathways driving differentiation in *T. cruzi* are still poorly understood. Among them, cAMP signaling has been linked to the development of infective forms

within the triatomine bug, a process called metacyclogenesis (Gonzales-Perdomo et al., 1988; Hamedi et al., 2015; Rangel-Aldao et al., 1988). cAMP has also been reported to mediate response to osmotic stress in *T. cruzi* (Docampo et al., 2013; King-Keller et al., 2010; Rohloff et al., 2004; Schoijet et al., 2011). In mammalian cells, the basic components of this signaling pathway are well defined, and the expression of these proteins in different microdomains determines spatiotemporal regulation of cAMP signals (Musheshe et al., 2018; Wang et al., 2022). We have recently identified two putative cAMP signaling microdomains in *T. cruzi*: the flagellar distal domain (flagellar tip) and the contractile vacuole complex (CVC), structures involved in cell adhesion and osmoregulation, respectively. However, just a few components of this pathway have been characterized in *T. cruzi* (Lander et al., 2021; Schoijet et al., 2019).

Calcium ion (Ca^{2+}) is another important intracellular signal in trypanosomatids that regulates essential cellular processes like host cell invasion (Moreno et al., 1994), differentiation (Lammel et al., 1996), osmoregulation (Rohloff et al., 2003), flagellar function (Engman et al., 1989), life/death decisions (Huang et al., 2013) and cell bioenergetics (Chiurillo et al., 2017; Chiurillo et al., 2020; Huang et al., 2013). As in vertebrate cells, cytosolic free Ca^{2+} concentration is strictly maintained in the range of 20-100 nm in different trypanosomatids (Moreno and Docampo, 2003). However, most types of plasma membrane Ca^{2+} channel orthologs are absent in these protozoans (Docampo and Huang, 2015). In the cytosol, soluble calcium-binding proteins sequester Ca^{2+} within different intracellular compartments. Some of them have been identified in the *T. cruzi* genome, but their role is still unknown.

The adaptation of the CRISPR/Cas9 system for genome editing to *T. cruzi*, has been a game change in the genetic manipulation of this parasite (Chiurillo and Lander, 2021; Lander and Chiurillo, 2019). Although the methods still show limitations when compared to other pathogenic protozoan such as *Toxoplasma gondii* or *Trypanosoma brucei*, the use of CRISPR/Cas9-based methods have significantly improved the ability to perform functional study of proteins by reverse genetic approaches in *T. cruzi*. The lack of efficient inducible methods for loss-of-function analyses in *T. cruzi* restrains the investigation of the role of essential genes in this parasite. The absence of the RNAi machinery in *T. cruzi* (DaRocha et al., 2004) and the apparent difficulty in adapting methods for inducible protein depletion

in this parasite, such as auxin-degron system, explain in part the mentioned limitations. Moreover, to the best of our knowledge, no large-scale or simultaneous multigene editing analysis have been reported in *T. cruzi*. Also, the lack of non-homologous end joining (NHEJ) machinery in trypanosomatids, makes necessary to use a donor DNA(s) to induce HDR after Cas9 cleavage for efficient gene editing, which limits large-scale approaches. Cloning-free systems to generate sgRNAs and DNA donor cassette(s) for delivery into *T. cruzi* cell lines engineered to constitutively express Cas9 and T7 RNA polymerase (T7RNAP) could enable systematic analysis of multiple genes, as successfully done in *Leishmania* species (Baker et al., 2021; Beneke et al., 2019; Damianou et al., 2020). Although the CRISPR/Cas9/T7RNAP-mediated method has been used in *T. cruzi* (Costa et al., 2018), an approach that can be easily scaled up for multigene editing in this parasite is still needed.

Taking advantage of the efficacy of CRISPR/Cas9-medited genome editing in *T. cruzi, in* this study we aimed at developing a fast and scalable strategy to identify essential genes when null mutants are non-viable. We used this strategy to generate knockout and tagged cell lines of three genes predicted to be involved in Ca^{2+} and cAMP signaling pathways: CAMK, FLAM6 and CC2CP. In addition, we performed a preliminary phenotype analysis of these mutants in *T. cruzi* epimastigotes.

MATERIAL AND METHODS

Chemicals and reagents

Alexa-conjugated secondary antibodies, HRP-conjugated secondary antibodies, Pierce ECL Western blotting substrate and BCA Protein Assay Kit were from Thermo Fisher Scientific Inc. Blasticidin S HCl was from Gibco. Puromycin was from Acros Organics (Fair Lawn, NJ). Anti-c-Myc (9E10) epitope tag monoclonal antibody was from Invitrogen. Benzonase® nuclease was from Novagen (EMD Millipore, Billerica, MA). GoTaq G2 Flexi DNA Polymerase, pGEM®-T Easy Vector Systems and T4 DNA Ligase were from Promega (Madison, WI). Restriction enzymes and Q5® High-Fidelity DNA Polymerase were from New England Biolabs (Ipswich, MA). Fluoromount-G® was from SouthernBiotech (Birmingham, AL). Nitrocellulose, polyacrylamide, and Precision Plus

Protein Dual Color protein standard were from Bio-Rad (Hercules, CA). DNA oligonucleotides were purchased from Integrated DNA Technologies, Inc. (Coraville, Iowa). *E. coli* DH5α Mix & Go competent cells, ZymoPURE Plasmid Midiprep kit, ZymoPURE Plasmid Miniprep kit were from Zymo Research (Irvine, CA). G418 Sulfate was from KSE Scientific (Durham, NC). Anti-tubulin mAb, mammalian cell protease inhibitor mixture (Sigma P8340), other protease inhibitors, and all other reagents of analytical grade were from Sigma (St. Louis, MO). The pMOTag23M vector (Oberholzer et al., 2006) was from Dr. Thomas Seebeck (University of Bern, Bern, Switzerland). The growth rate of epimastigotes was determined by counting cells in a Neubauer chamber.

Cell culture

T. cruzi Y strain epimastigotes were cultured in liver infusion tryptose (LIT) medium containing 10% heat-inactivated fetal bovine serum (FBS) at 28°C (Bone and Steinert, 1956) T7/Cas9 cell line was maintained in medium containing 250 μg/ml G418. Mutant cell lines with single deleted allele were maintained in medium containing 250 μg/ml G418 and 5 μg/ml puromycin, while for KO cell lines 10 μg/ml blasticidin was additionally added.

***In silico* analysis**

Nucleotide sequences of *T. cruzi* Y strain *AEK1* (TcYC6_0120630), *CAMK* (TcYC6_0047690), *FLAM6* (TcYC6_0109380) and *CC2CP* (TcYC6_0079900) genes were retrieved from TriTrypDB genome data (tritrypdb.org). Prediction of protein domains of CAMK, FLAM6 and CC2CP amino acid sequences was made using web servers: https://ebi.ac.uk/interpro/ and https://prosite.expasy.org/scanprosite/. Selection of protospacers for knockout and tagging strategies was performed using EuPaGDT (eukaryotic pathogen CRISPR guide RNA/DNA design tool; http://grna.ctegd.uga.edu) (Peng and Tarleton, 2015).

Generation of a *T. cruzi* cell line stably expressing T7 RNA Polymerase and Cas9.

To generate a *T. cruzi* cell line that constitutively expresses both T7RNAP and Cas9 nuclease (T7RNAP/Cas9), *T. cruzi* Y strain epimastigotes were transfected with circular pTREX-n-T7RNAP/Cas9 plasmid, which was created by cloning the T7RNAP gene into pTREXn/Cas9 vector (Lander et al., 2015) upstream the Cas9-HA-GFP ORF, and interspaced by the *T. cruzi* trans-splicing region *HX1* (Fig. S1A). Clonal populations of

parasites were obtained in 96-well pates by limiting dilutions in conditioned medium.

Design and PCR-amplification of sgRNA templates

The 124-bp DNA templates for sgRNA transcription were designed as previously reported (Bassett and Liu, 2014). The PCR contains a forward primer which is target-specific and includes the T7 polymerase binding site, the 20-nt of the target sequence or protospacer, and a region complementary to a common reverse primer (RvG00) containing the remaining the sequence of the sgRNA (Table S1). sgRNA templates were amplified using Q5® High-Fidelity DNA polymerase and 10 μM of each Fw-sgRNA and RvG00 primers under the following conditions: a first denaturation step of 98°C for 30 sec, followed by 15 cycles of 98°C for 10 s, 55°C for 20 s, and 72°C for 15 s, then 25 cycles of 98 °C for 10 s, and 72°C for 20 s followed by a final extension 72 °C for 2 min.

Endogenous C-terminal gene tagging

The choice of the target sequence to design sgRNA template to perform CRISPR/Cas9-mediated endogenous C-terminal tagging of the genes analyzed in this work was done as previously described (Lander et al., 2016b; Lander et al., 2017). DNA donor cassette containing the 3xc-Myc tag sequence and the puromycin resistance gene to induce homology-directed repair was amplified using the pMOTag23M vector (Oberholzer et al., 2006) as template. Primers to amplify by PCR the DNA donor cassette were designed to be 60-nt long, including the common nucleotide sequences to anneal to the pMOTag23M plasmid, and 39-nt and 34-nt target-specific sequences in the forward and reverse primers (Fw/Rv CTag), respectively (Table S1). *T. cruzi* T7/Cas9 epimastigotes were co-transfected with the sgRNA template and the DNA donor cassette, and then cultured for 3 weeks with G418 and puromycin for selection of resistant parasites. Endogenous gene tagging was verified by PCR from gDNA using primers Fw/Rv CTag check (Table S1) and by Western blot analysis using total protein extracts.

CRISPR-Cas9 mediated gene deletion

Plasmids used as DNA template in PCR reactions to generate donor DNAs for gene deletion/disruption strategies were obtained by amplifying blasticidin S deaminase (*BSD*) and puromycin-N-acetyltrasnferase (*PAC*) genes and cloning them individually into pGEM®-T Easy Vector (Promega). These plasmids were named p*BSD* and p*PAC*, respectively. The reverse primers to amplify both genes included GTGA as four last

nucleotides, therefore GTGA is the 3'end of *BSD* and *PAC* genes. For PCR-amplification of resistance cassettes we used 60-nt primers that were designed as follows (Table S1): The forward primers contain a 40-nt 5'UTR-containing homologous region (HR) plus 20 nucleotides of the plasmid backbone including the start codon (5'-GCCGCGGGAATTCGATTATG-3'). The reverse primers consist of 37 nucleotides of the 3'UTR-containing HR followed by 23 nucleotides of the plasmid backbone and the four last nucleotides of the antibiotic resistance genes, including the stop codon (5'-CGCGAATTCACTAGTGATTTCAC-3'). Homology donor targeting sequences in forward/reverse primers were designed by manual verification of the appropriate sequence in TriTrypDB. To amplify the donor DNA cassettes, 30 ng circular p*BSD* and p*PAC* plasmid DNA, 0.4 μM of 60-nt gene-specific forward and reverse primers, and 5% (v/v) DMSO when amplifying PAC cassette, and 1.5 U of GoTaq G2 Flexi DNA Polymerase, were mixed in 50 μl total volume. PCR steps were 2 min at 95°C, followed by 15 cycles of 20 s at 95°C, 20 s at 60°C, 55 s at 72°C, then other 25 cycles of 20 s at 95°C, 1 min at 72°C, followed by a final elongation step for 5 min at 72°C. Sizes of donor DNA cassettes are 515 bp and 715 bp for *BSD* and *PAC* resistant markers, respectively.

To generate single-KO or null mutant cell lines for each gene of interest we co-transfected *T. cruzi* T7/Cas9 epimastigotes with the sgRNA template and one (puromycin) or two (puromycin and blasticidin) DNA donor cassettes, respectively. Transfected parasites were cultured for 3-5 weeks in the presence of G418 and puromycin, or G418, puromycin and blasticidin, for selection of single or double-resistant parasites, respectively. When double KO cells were not obtained by transfecting with two DNA donor cassettes simultaneously, stable confirmed single-KO cells were subjected to a second round of transfection including the sgRNA template and the blasticidin resistance cassette. Gene disruption was verified using gDNA from mutant parasites by PCR using primers Fw/Rv-KO check (Table S1).

Cell transfections

T. cruzi Y strain epimastigotes expressing T7 RNAP and Cas9 were transfected as described previously (Chiurillo et al., 2017). Briefly, *T. cruzi* epimastigotes in early exponential phase (4 x 10^7 cells) were washed with PBS, pH 7.4, at room temperature (RT) and transfected in ice-cold CytoMix (120 mM KCl, 0.15 mM $CaCl_2$, 10 mM K_2HPO_4, 25

mM HEPES, 2 mM EDTA, 5 mM $MgCl_2$, pH 7.6) containing 25 μg of each plasmid construct and 25 μg of donor DNA in 4-mm electroporation cuvettes with three pulses (1500 volts, 25 microfarads) delivered by a Gene Pulser Xcell™ Electroporation System (Bio-Rad). Transfected epimastigotes were cultured in LIT medium supplemented with 20% heat-inactivated FBS until stable cell lines were obtained. When needed, the antibiotic (concentration) used for drug selection and maintenance was 250 μg/ml G418, 10 μg/ml blasticidin or 5 μg/ml puromycin.

Western blot analysis

Western blots were carried as described previously (Lander et al., 2010). Briefly, parasites were harvested and washed twice in PBS and subsequently resuspended in radio-immunoprecipitation assay buffer (RIPA: 150 mM NaCl, 20 mM Tris-HCl, pH 7.5, 1 mM EDTA, 1% SDS, 0.1% Triton X-100) plus a mammalian cell protease inhibitor mixture (diluted 1:250), 1 mM phenylmethylsulfonyl fluoride, 2.5 mM tosyl phenylalanyl chloromethyl ketone (TPCK), 100 M *N*-(*trans*-epoxysuccinyl)-L- leucine 4-guanidinobutylamide (E64), and Benzonase Nuclease (25 units/ml of culture). The cells were then incubated for 1 h on ice and protein concentration was determined by BCA protein assay. Thirty micrograms of protein from each cell lysate were mixed with 6 Laemmli sample buffer (125 mM Tris-HCl, pH 7, 10% (w/v) β-mercaptoethanol, 20% (v/v) glycerol, 4.0% (w/v) SDS, 4.0% (w/v) bromphenol blue) before application to 10% SDS-polyacrylamide gels. Electrophoresed proteins were transferred onto nitrocellulose membranes with a Bio-Rad Trans-Blot® Turbo™ Transfer System. Membranes were blocked with 5% nonfat dried skim milk in PBS-T (PBS containing 0.1% v/v Tween 20) overnight at 4 °C. Next, blots were incubated for 1 h, at RT, with a primary antibody (monoclonal anti-c-Myc-tag [1:1000] and monoclonal anti-tubulin [1:40,000]). After three washes with PBS-T, blots were incubated with the secondary antibody (goat anti-mouse IgG HRP-conjugated antibody, diluted [1:10,000]). Membranes were washed three times with PBS-T, then blots were incubated with Pierce ECL Plus Substrate and images were obtained and processed with a ChemiDoc Imaging System (Bio-Rad). Blot densitometry analyses were performed with ImageJ v1.48 software.

Immunofluorescence analysis

Cells were washed with PBS and fixed with 4% paraformaldehyde in PBS for 1 h at RT.

Cells were allowed to adhere to poly-L-lysine-coated coverslips and then permeabilized for 5 min with 0.1% Triton X-100. Permeabilized cells were blocked with PBS containing 3% BSA, 1% fish gelatin, 50 mM NH_4Cl, and 5% goat serum overnight at 4 °C. Then, cells were incubated with a primary antibody (monoclonal anti-c-Myc-tag [1:100]), diluted in 1% BSA in PBS (pH 8.0) for 1 h at RT. Cells were washed three times with 1% BSA in PBS (pH 8.0), and then incubated for 1 h at RT in the dark with Alexa Fluor 488 or Alexa Fluor 546-conjugated goat anti-mouse secondary antibodies (1:1000). Then, cells were washed and mounted on slides using Fluoromount-G mounting medium containing 5 μg/ml of 4,6-diamidino-2-phenylindole (DAPI) to stain DNA. Controls were done as described above but in the absence of a primary antibody. Differential interference contrast and fluorescence optical images were captured with a 100× objective in an Upright Motorized Fluorescence Microscope ECLIPSE Ni-E (Nikon) with NIS-Elements Advanced Research Package for 6D Image Acquisition and Analysis, and 2D fast deconvolution software.

RESULTS

To adapt the CRISPR/Cas9 methodology for large-scale genetic screenings, we transfected *T. cruzi* Y strain epimastigotes with pTREX-n-T7RNAP/Cas9 construct (Fig S1A) to generate a lineage that constitutively expresses Cas9 and T7RNAP, in which genome editing can be achieved in a cloning-free strategy where both, sgRNA (with an upstream T7RNAP promoter) and donor DNA(s), are co-transfected as PCR products. pTREX vector integrates into the *T. cruzi* genome (Vazquez and Levin, 1999), allowing the stable expression of T7RNAP and Cas9 genes. Expression of Cas9 in a clonal population was confirmed by western blot analysis and by direct observation of *T. cruzi* cells with green nuclei under fluorescence microscopy. T7RNAP/Cas9 epimastigotes showed no difference in growth compared to control (pTREXn empty vector) parasites (Fig S1B).

To generate a null mutant population using the T7RNAP/Cas9 system in a single electroporation round it is necessary to transfect cells with 2 donor DNAs, each one containing a different resistance marker. Therefore, we generated a set of 2 plasmids using the pGEM®-T Easy Vector Systems (Promega) as backbone to clone blasticidin and

puromycin resistance genes (p*BSD* and p*PAC*, respectively). The design allows to use a single pair of primers to amplify any of the resistance cassettes. Primers to amplify by PCR the DNA donor cassettes were designed to be 60-nt long, including the common nucleotide sequences to anneal to p*BSD* and p*PAC,* and 40-nt and 37-nt target-specific HR sequence in the forward and reverse primers (Fw/Rv-KO), respectively, although primers with 30 nt of HR were also tested showing similar efficiency. Our strategy is based on choosing the HR in the 5' and 3' UTRs right flanking the start and stop codon of the gene of interest (GOI), respectively (Fig. 1A). In the present study we followed a two-step strategy for gene deletion: 1) in a first round of transfections, we transfected in duplicates *T. cruzi* epimastigotes with one specific sgRNA template and two (Fig. 1A) or one donor DNAs (puromycin resistance cassette) for HDR; 2) if the KO cell line was not obtained, in a second round of transfection we delivered the sgRNA template plus the donor DNA with the blasticidin resistance cassette in a stable single allele deletion mutant cell line (single knockout) generated in the first round of transfections.

To validate the efectiveness of our T7/Cas9 system we attempted to generate a null mutant cell line of the AGC essential kinase 1 (*TcAEK1*; TriTrypDB ID: TcYC6_0120630; 1179 bp). *AEK1* in *T. cruzi* is essential for epimastigote proliferation, trypomastigote host cell invasion, and amastigote replication, as well as involved in cytokinesis regulation (Chiurillo et al., 2021). Using an efficient CRISPR/Cas9 method we adapted for *T. cruzi* (Chiurillo et al., 2017; Chiurillo et al., 2019; Chiurillo et al., 2020; Lander and Chiurillo, 2019; Lander et al., 2016a; Lander et al., 2015; Negreiros et al., 2021), which involves the constitutive expression of Cas9 and the sgRNA, it was only possible to generate a single *TcAEK1* allele deletion cell line. In this previous work, several attempts with different strategies demonstrated the essentiality of *TcAEK1* because it was not possible to obtain null mutants. Consistently, here we were just able to obtain a *TcAEK1* single KO (*TcAEK1-SKO*) cell line (Fig. 1B), since both attempts, transfecting with 2 resistance cassettes at the same time or in two sequential rounds of transfections, were unsuccessful in generating null mutant cells for this gene. As expected, cells showing a defect in cytokinesis were observed in *TcAEK1-SKO* epimastigotes (Fig. 1C).

We next investigated a putative Ca^{2+}/calmodulin-dependent protein kinase (*TcCAMK*; TriTrypDB ID: TcYC6_0047690; 1638 bp), whose ortholog in *T. brucei* is an essential

gene involved in cytokinesis (Jones et al., 2014). Initially we evaluated the T7RNAP/Cas9 system for endogenous C-terminal tagging method by inserting the c-Myc epitope tag sequence into the 3' end of *TcCAMK* gene. The strategy consisted in co-transfecting T7RNAP/Cas9 epimastigotes with a specific sgRNA template targeting the 3' end of *TcCAMK* gene with a specific DNA donor molecule for each gene amplified from the pMOTag23M vector (Lander et al., 2017; Oberholzer et al., 2006). In general, this strategy will tag one of the alleles of the gene (Fig. 2A). Using this method *TcCAMK* was efficiently tagged at the endogenous locus with a 3xc-Myc tag, as confirmed by PCR (Fig. 2B), and western blot analysis using anti-c-Myc antibodies, detecting a band of the predicted size (67 kDa) (Fig. 2C). Immunofluorescence analysis (IFA) of the mutants showed that TcCAMK has a cytosolic localization in *T. cruzi* epimastigotes (Fig. 2D). Subsequently, we generated *TcCAMK-KO* epimastigotes, as confirmed by PCR (Fig. 2E), by transfecting *T. cruzi* epimastigotes simultaneously with *BSD* and *PAC* resistance cassettes. *TcCAMK-KO* epimastigotes showed no difference in growth rate compared to control parasites (Fig. 2F), indicating that this putative *TcCAMK* gene is not essential at least for the epimastigote stage of *T. cruzi.*

Using similar strategies, we studied the subcellular localization of TcFLAM6 (Flagellar Member 6, TriTrypDB: TcYC6_0109380, 4191 bp), whose ortholog was identified as a flagellar protein of *T. brucei* procyclic forms (Subota et al., 2014) and it is predicted to have two cNMP binding motifs (Jager et al., 2014). Fig. 3 shows the efficient tagging of *TcFLAM6* with 3xc-Myc at the endogenous locus, as detected by PCR, western blot analysis (predicted 162 kDa band) and IFA (Fig. 3A-C). Interestingly, TcFLAM6 localized to the proximal region of the flagellum (Fig. 3C). *TcFLAM6-KO* cell line was generated after transfecting stable puromycin-resistant *TcFLAM6-SKO* epimastigotes with the sgRNA template and *BSD* donor DNA, since no viable *TcFLAM6* null mutants were obtained when the two donor resistance cassettes were delivered ate the same time. Replacement of both alleles in *TcFLAM6-KO* cells was confirmed by PCR (Fig. 3D). Moreover, *TcFLAM6-KO* epimastigotes showed a significant lower growth rate in LIT medium in the exponential phase of growth, compared to control cells (Fig. 3E).

Finally, we investigated a putative cAMP protein (TriTrypDB: TcYC6_0079900), which is 5076-bp gene and whose predicted protein product (~187 kDa) contains two N-terminal

cNMP binding motifs (CBD) and three C2 domains (calcium binding motifs) in the C-terminal region, according to InterPro (ebi.ac.uk/interpro/). We named this protein as Cyclic nucleotide-binding domain/C2 domain-containing protein (*TcCC2CP*). Then, we generated a *TcCC2CP* endogenous C-terminal tagged cell line, as confirmed by PCR and western blot analysis (Fig. 4A,B). *TcCC2CP*-3xc-Myc protein shows cytosolic localization by IFA, with a pattern probably compatible with cytoplasmic organelles or endomembranes (Fig. 4C). Furthermore, no populations of *TcCC2CP* null mutants were recovered after simultaneous transfection with two donor DNA cassettes or after performing a second round of transfection using *TcCC2CP-SKO* cell line, which could be easily generated (Fig. 4D). Interestingly, *TcCC2CP-SKO* epimastigotes exhibited a growth rate in LIT medium significantly lower than that of the parental T7RNAP/Cas9 cell line (Fig. 4E).

DISCUSSION

In *T. cruzi* the CRISPR/Cas9 strategy involving co-transfection of epimastigotes with a vector for constitutive expression of Cas9 and sgRNA, plus a donor DNA cassette to induce HDR, has been successfully used to generate gene knockout mutants as well for endogenous gene tagging (Bertolini et al., 2019; Chiurillo et al., 2021; Chiurillo et al., 2019; Chiurillo et al., 2020; Lander and Chiurillo, 2019; Lander et al., 2016b; Lander et al., 2015; Negreiros et al., 2021). However, this strategy can exhibit some drawbacks, such as long selection time to obtain stable KO cell lines and the need of cloning the sgRNA into the Cas9/pTREX-n vector before transfection. Moreover, the constitutive expression of Cas9 and sgRNA has been associated with off target effects (Hsu et al., 2013). Other successful CRISPR/Cas9-mediated genome editing methods used in *T. cruzi* involve transfection of *in vitro* transcribed sgRNA, either with constitutive expression of Cas9 (Burle-Caldas et al., 2022; Marcelino et al., 2023; Marek et al., 2021; Peng et al., 2014) or introduced as RNP complex with recombinant Cas9 (Saenz-Garcia et al., 2021; Soares Medeiros et al., 2017). In the latter cases, although the transient expression of the sgRNA can be beneficial (and also the transient expression of Cas9 when they are transfected as RNP complex), these strategies are not suitable for large scale editing of genes.

CRISPR/Cas9 strategies involving transfection of epimastigotes stably expressing Cas9 and T7 RNA polymerase, which drives sgRNA transcription *in vivo* from DNA templates generated by PCR, plus donor cassette(s) for HDR have significantly boosted reverse genetics studies in *Leishmania* (Beneke et al., 2017; Damianou et al., 2020; Espada et al., 2021; Grewal et al., 2019; Jones et al., 2018; Martel et al., 2017; Turra et al., 2021), and it was also used in *T. brucei* (Beneke et al., 2017*)*. This cloning-free strategy has substantially increased the number of genes studied in different *Leishmania* species, mainly because the method can be used for simultaneously editing multiple genes in a large-scale format (Baker et al., 2021; Beneke et al., 2019; Damianou et al., 2020). Moreover, the transient expression of the sgRNA represents another advantage of the method to avoid off-target effects. This CRISPR/Cas9/T7RNAP-mediated genome editing strategy has been used in *T. cruzi* for gene tagging, and for ablation of a non-essential gene (GP72) (Costa et al., 2018). The method we have developed in this work shows some differences with the one used by Costa et al. (Costa et al., 2018): 1) T7RNAP/Cas9 expressing cell line was generated by transfecting both genes cloned into the *T. cruzi*-specific expression vector pTREX-n, instead of pLew13 plasmid; 2) epimastigotes are transfected with a sgRNA template instead of two; 3) Both alleles of the GOI are replaced by two resistance markers, preserving the endogenous UTRs to regulate their expression. Given the absence of the RNAi machinery in *T. cruzi*, a cloning-free CRISPR/Cas9/T7RNAP-mediated strategy seems to be the most appropriate approach so far to perform large-scale gene editing in this parasite. Furthermore, when a gene knockout attempt fails with any genome editing method, it often leads to the conclusion that the gene is “essential”. However, possible technical issues such as potential mismatches in the sequences of the protospacer and the protospacer adjacent motif (PAM) or incorrect assembly of the reference genome, can make the locus non-editable. Instead of repeating transfections or designing new sgRNA and homology regions (HRs), in this work per each GOI we transfected parasites with either one or two resistance cassettes, so that if double resistant parasites were not obtained, stable single KO cells were transfected with another DNA resistance marker in a second round of transfection. Our previous experience indicates that single KO cell lines can be generated even in cases in which mutant epimastigotes exhibit lower growth rates compared with parental cells (Chiurillo et al., 2021; Dos Santos et al., 2021; Lander et al.,

2018). Following the mentioned strategy as a routine for gene ablation we were able to: 1) obtain null mutants faster than performing multiple attempts to delete both alleles at the same time, 2) be more certain when concluding that a gene is essential in *T. cruzi* epimastigotes. In addition, considering the limited number of effective resistance markers available for selection of *T. cruzi* mutants, endogenous genes could be restored in KO parasites, as the hygromycin resistance marker is still available for selection of add back transfectants.

In this work we analyzed three different genes, for which null mutant epimatigotes were obtained in the first attempt for *TcCAMK*, or after transfecting single null parasites for *TcFLAM6*. However, we failed to obtain *TcCC2CP-KO* cells even after performing a second round of transfection using the *TcCC2CP-SKO* cell line. Interesting, the results correlate with fact that *TcFLAM6-KO* and *TcCC2CP-SKO* epimastigotes exhibited lower growth rates than the parental cell line, which suggests both genes are important for *T. cruzi* in this developmental stage.

Calcium/calmodulin-dependent protein kinases (CAMK) comprise a group of Serine/Threonine protein kinases that are regulated by allosteric activation with Calcium/calmodulin when the intracellular concentration of Ca^{2+} increases. The CAMK group (which includes the AMPK) is poorly represented in trypanosomatid genomes compared to the human kinome (Parsons et al., 2005). In the *T. cruzi* YC6 genome available in TriTrypDB we found 15 putative CAMK and CAMKL (CAMK-like) genes, among which we are particularly interested in one (TriTrypDB ID: TcYC6_0047690), whose ortholog in *T. brucei* (TriTrypDB ID: Tb927.7.6220) was previously assessed in a kinome-wide RNAi library (Jones et al., 2014). In that work, the knockdown of this *TbCAMK* induced growth arrest and cytokinesis defects in bloodstream forms. However, different to *TbCAMK*-downregulated cells, *TcCAMK-KO* epimastigotes did not exhibit morphological alterations or a growth defect, suggesting that the *T. cruzi* ortholog is not essential at least in the epimastigote stage.

In a proteomic analysis of flagella of *T. brucei* procyclic forms were identified eight novel proteins, FLAM1 to 8 (Subota et al., 2014), which were recently also detected in an APEX-based proximity proteomics approach in the same stage of this parasite (Velez-Ramirez et al., 2021). Remarkably, FLAM6 contains two CBDs suggesting that this protein could bind

cAMP and eventually have a role in the flagellar function as an effector of this second messenger in trypanosomatids. Here, we observed that TcFLAM6 is localized in the proximal third of the epimastigote's flagellum, similar to what was observed in *T. brucei* procyclic forms in which TbFLAM6 is restricted to the proximal portion of the flagellum, no matter its length (Subota et al., 2014). The fact that in procyclic forms, TbFLAM6 is restricted to the proximal half of the axoneme at all stages of formation of the new flagellum, even when the flagellum starts to elongate, suggests a strict spatiotemporal regulation of FLAM6 synthesis and flagellar assembly (Subota et al., 2014). Moreover, *TcFLAM6-KO* epimastigotes exhibited a lower growth rate in the exponential phase compared to parental cells, which in addition to the unsuccessful generation of a null mutant in a first round of transfection with two resistance markers, confirms the importance of this gene in *T. cruzi* epimastigotes. Interestingly, in a proximity-dependent biotinylation approach of flagellar proteins of *T. cruzi*, unlike other FLAM proteins (FLAM1,2,3,5,7 and 8), TcFLAM6 was only detected in epimastigotes and not in intracellular amastigotes (Won et al., 2023).

CC2CP predicted CBDs were previously analyzed *in silico* in a bioinformatic identification of cyclic nucleotide binding proteins in *T. cruzi* (Jager et al., 2014). Interestingly this protein also has C2 domains, which are structural domains involved in targeting proteins to cell membranes in a calcium-dependent manner (Zhang and Aravind, 2010). Furthermore, transcriptomic analyses revealed higher expression levels of *TcCC2CP* in metacyclic trypomastigotes in *T. cruzi* Brazil and Dm28c strains (Minning et al., 2009; Smircich et al., 2015). In this work *TcCC2CP* could not be ablated, and *TcCC2CP-SKO* parasites exhibited a growth defect in epimastigotes, suggesting that *TcCC2CP* is an essential gene in epimastigotes, and could play an important role in other developmental stages of *T. cruzi.* Many proteins containing C2 domains are implicated in signal transduction or membrane trafficking (Nalefski and Falke, 1996). The presence of both CBD and C2 domains and the subcellular localization observed by IFA suggests that TcCC2CP is a component of the cAMP signaling pathway coupled with molecules or organelle trafficking.

In summary, the gene editing strategies developed in this work expand the toolkit available to perform reverse genetics in *T. cruzi*. Particularly, the T7RNAP/Cas9 system generated

and the strategy used to obtain gene deletion mutants, could facilitate large-scale gene analyses in this parasite. Our preliminary study of two putative cAMP binding proteins, TcFLAM6 and TcCC2CP, the latter containing also predicted C2 domains, suggest the importance of them at least in the epimastigote stage of *T. cruzi*. Further work, evaluating the expression pattern, interactome and role of these proteins in other developmental stages are necessary to elucidate their importance in *T. cruzi* life cycle.

Acknowledgements

Thomas Seebeck for the pMOTag23M vector. Funding for this work was provided by the National Institute of Allergy and Infectious Diseases of the National Institutes of Health (Award number R00AI137322 to N. Lander) and the Latino Faculty Association of University of Cincinnati (2023 LFA award to M.A. Chiurillo). A. Raja was an UPRISE awardee at the University of Cincinnati.

References

Baker, N., Catta-Preta, C.M.C., Neish, R., Sadlova, J., Powell, B., Alves-Ferreira, E.V.C., Geoghegan, V., Carnielli, J.B.T., Newling, K., Hughes, C.*, et al.* (2021). Systematic functional analysis of Leishmania protein kinases identifies regulators of differentiation or survival. Nat Commun *12*, 1244.

Bassett, A., and Liu, J.L. (2014). CRISPR/Cas9 mediated genome engineering in Drosophila. Methods *69*, 128-136.

Beneke, T., Demay, F., Hookway, E., Ashman, N., Jeffery, H., Smith, J., Valli, J., Becvar, T., Myskova, J., Lestinova, T.*, et al.* (2019). Genetic dissection of a Leishmania flagellar proteome demonstrates requirement for directional motility in sand fly infections. PLoS Pathog *15*, e1007828.

Beneke, T., Madden, R., Makin, L., Valli, J., Sunter, J., and Gluenz, E. (2017). A CRISPR Cas9 high-throughput genome editing toolkit for kinetoplastids. R Soc Open Sci *4*, 170095.

Bertolini, M.S., Chiurillo, M.A., Lander, N., Vercesi, A.E., and Docampo, R. (2019). MICU1 and MICU2 Play an Essential Role in Mitochondrial Ca(2+) Uptake, Growth, and Infectivity of the Human Pathogen Trypanosoma cruzi. mBio *10*.

Bone, G.J., and Steinert, M. (1956). Isotopes incorporated in the nucleic acids of Trypanosoma mega. Nature *178*, 308-309.

Bonney, K.M., Luthringer, D.J., Kim, S.A., Garg, N.J., and Engman, D.M. (2019). Pathology and Pathogenesis of Chagas Heart Disease. Annu Rev Pathol *14*, 421-447.

Burle-Caldas, G.A., Dos Santos, N.S.A., de Castro, J.T., Mugge, F.L.B., Grazielle-Silva, V., Oliveira, A.E.R., Pereira, M.C.A., Reis-Cunha, J.L., Dos Santos, A.C., Gomes, D.A., *et al.* (2022). Disruption of Active Trans-Sialidase Genes Impairs Egress from Mammalian Host Cells and Generates Highly Attenuated Trypanosoma cruzi Parasites. mBio *13*, e0347821.

Chiurillo, M.A., Jensen, B.C., and Docampo, R. (2021). Drug Target Validation of the Protein Kinase AEK1, Essential for Proliferation, Host Cell Invasion, and Intracellular Replication of the Human Pathogen Trypanosoma cruzi. Microbiol Spectr *9*, e0073821.

Chiurillo, M.A., and Lander, N. (2021). The long and winding road of reverse genetics in Trypanosoma cruzi. Microb Cell *8*, 203-207.

Chiurillo, M.A., Lander, N., Bertolini, M.S., Storey, M., Vercesi, A.E., and Docampo, R. (2017). Different Roles of Mitochondrial Calcium Uniporter Complex Subunits in Growth and Infectivity of Trypanosoma cruzi. mBio *8*.

Chiurillo, M.A., Lander, N., Bertolini, M.S., Vercesi, A.E., and Docampo, R. (2019). Functional analysis and importance for host cell infection of the Ca(2+)-conducting subunits of the mitochondrial calcium uniporter of Trypanosoma cruzi. Mol Biol Cell *30*, 1676-1690.

Chiurillo, M.A., Lander, N., Vercesi, A.E., and Docampo, R. (2020). IP3 receptor-mediated Ca(2+) release from acidocalcisomes regulates mitochondrial bioenergetics and prevents autophagy in Trypanosoma cruzi. Cell Calcium *92*, 102284.

Costa, F.C., Francisco, A.F., Jayawardhana, S., Calderano, S.G., Lewis, M.D., Olmo, F., Beneke, T., Gluenz, E., Sunter, J., Dean, S., *et al.* (2018). Expanding the toolbox for Trypanosoma cruzi: A parasite line incorporating a bioluminescence-fluorescence dual reporter and streamlined CRISPR/Cas9 functionality for rapid in vivo localisation and phenotyping. PLoS Negl Trop Dis *12*, e0006388.

Damianou, A., Burge, R.J., Catta-Preta, C.M.C., Geoghegan, V., Nievas, Y.R., Newling, K., Brown, E., Burchmore, R., Rodenko, B., and Mottram, J.C. (2020). Essential roles for deubiquitination in Leishmania life cycle progression. PLoS Pathog *16*, e1008455.

DaRocha, W.D., Otsu, K., Teixeira, S.M., and Donelson, J.E. (2004). Tests of cytoplasmic RNA interference (RNAi) and construction of a tetracycline-inducible T7 promoter system in Trypanosoma cruzi. Mol Biochem Parasitol *133*, 175-186.

Docampo, R., and Huang, G. (2015). Calcium signaling in trypanosomatid parasites. Cell Calcium *57*, 194-202.

Docampo, R., Jimenez, V., Lander, N., Li, Z.H., and Niyogi, S. (2013). New insights into roles of acidocalcisomes and contractile vacuole complex in osmoregulation in protists. Int Rev Cell Mol Biol *305*, 69-113.

Dos Santos, G.R.R., Rezende Leite, A.C., Lander, N., Chiurillo, M.A., Vercesi, A.E., and Docampo, R. (2021). Trypanosoma cruzi Letm1 is involved in mitochondrial Ca(2+) transport, and is essential for replication, differentiation, and host cell invasion. FASEB J *35*, e21685.

Engman, D.M., Krause, K.H., Blumin, J.H., Kim, K.S., Kirchhoff, L.V., and Donelson, J.E. (1989). A novel flagellar Ca2+-binding protein in trypanosomes. J Biol Chem *264*, 18627-18631.

Espada, C.R., Quilles, J.C., Jr., Albuquerque-Wendt, A., Cruz, M.C., Beneke, T., Lorenzon, L.B., Gluenz, E., Cruz, A.K., and Uliana, S.R.B. (2021). Effective Genome Editing in Leishmania (Viannia) braziliensis Stably Expressing Cas9 and T7 RNA Polymerase. Front Cell Infect Microbiol *11*, 772311.

Gonzales-Perdomo, M., Romero, P., and Goldenberg, S. (1988). Cyclic AMP and adenylate cyclase activators stimulate Trypanosoma cruzi differentiation. Exp Parasitol *66*, 205-212.

Grewal, J.S., Catta-Preta, C.M.C., Brown, E., Anand, J., and Mottram, J.C. (2019). Evaluation of clan CD C11 peptidase PNT1 and other Leishmania mexicana cysteine peptidases as potential drug targets. Biochimie *166*, 150-160.

Hamedi, A., Botelho, L., Britto, C., Fragoso, S.P., Umaki, A.C., Goldenberg, S., Bottu, G., and Salmon, D. (2015). In vitro metacyclogenesis of Trypanosoma cruzi induced by starvation correlates with a transient adenylyl cyclase stimulation as well as with a

constitutive upregulation of adenylyl cyclase expression. Mol Biochem Parasitol *200*, 9-18.

Hsu, P.D., Scott, D.A., Weinstein, J.A., Ran, F.A., Konermann, S., Agarwala, V., Li, Y., Fine, E.J., Wu, X., Shalem, O.*, et al.* (2013). DNA targeting specificity of RNA-guided Cas9 nucleases. Nat Biotechnol *31*, 827-832.

Huang, G., Vercesi, A.E., and Docampo, R. (2013). Essential regulation of cell bioenergetics in Trypanosoma brucei by the mitochondrial calcium uniporter. Nat Commun *4*, 2865.

Jager, A.V., De Gaudenzi, J.G., Mild, J.G., Mc Cormack, B., Pantano, S., Altschuler, D.L., and Edreira, M.M. (2014). Identification of novel cyclic nucleotide binding proteins in Trypanosoma cruzi. Mol Biochem Parasitol *198*, 104-112.

Jones, N.G., Catta-Preta, C.M.C., Lima, A., and Mottram, J.C. (2018). Genetically Validated Drug Targets in Leishmania: Current Knowledge and Future Prospects. ACS Infect Dis *4*, 467-477.

Jones, N.G., Thomas, E.B., Brown, E., Dickens, N.J., Hammarton, T.C., and Mottram, J.C. (2014). Regulators of Trypanosoma brucei cell cycle progression and differentiation identified using a kinome-wide RNAi screen. PLoS Pathog *10*, e1003886.

King-Keller, S., Li, M., Smith, A., Zheng, S., Kaur, G., Yang, X., Wang, B., and Docampo, R. (2010). Chemical validation of phosphodiesterase C as a chemotherapeutic target in Trypanosoma cruzi, the etiological agent of Chagas' disease. Antimicrob Agents Chemother *54*, 3738-3745.

Lammel, E.M., Barbieri, M.A., Wilkowsky, S.E., Bertini, F., and Isola, E.L. (1996). Trypanosoma cruzi: involvement of intracellular calcium in multiplication and differentiation. Exp Parasitol *83*, 240-249.

Lander, N., Bernal, C., Diez, N., Anez, N., Docampo, R., and Ramirez, J.L. (2010). Localization and developmental regulation of a dispersed gene family 1 protein in Trypanosoma cruzi. Infect Immun *78*, 231-240.

Lander, N., and Chiurillo, M.A. (2019). State-of-the-art CRISPR/Cas9 Technology for Genome Editing in Trypanosomatids. J Eukaryot Microbiol *66*, 981-991.

Lander, N., Chiurillo, M.A., Bertolini, M.S., Storey, M., Vercesi, A.E., and Docampo, R. (2018). Calcium-sensitive pyruvate dehydrogenase phosphatase is required for energy

metabolism, growth, differentiation, and infectivity of Trypanosoma cruzi. J Biol Chem *293*, 17402-17417.

Lander, N., Chiurillo, M.A., and Docampo, R. (2016a). Genome Editing by CRISPR/Cas9: A Game Change in the Genetic Manipulation of Protists. J Eukaryot Microbiol *63*, 679-690.

Lander, N., Chiurillo, M.A., and Docampo, R. (2021). Signaling pathways involved in environmental sensing in Trypanosoma cruzi. Mol Microbiol *115*, 819-828.

Lander, N., Chiurillo, M.A., Storey, M., Vercesi, A.E., and Docampo, R. (2016b). CRISPR/Cas9-mediated endogenous C-terminal Tagging of Trypanosoma cruzi Genes Reveals the Acidocalcisome Localization of the Inositol 1,4,5-Trisphosphate Receptor. J Biol Chem *291*, 25505-25515.

Lander, N., Chiurillo, M.A., Vercesi, A.E., and Docampo, R. (2017). Endogenous C-terminal Tagging by CRISPR/Cas9 in Trypanosoma cruzi. Bio Protoc *7*.

Lander, N., Li, Z.H., Niyogi, S., and Docampo, R. (2015). CRISPR/Cas9-Induced Disruption of Paraflagellar Rod Protein 1 and 2 Genes in Trypanosoma cruzi Reveals Their Role in Flagellar Attachment. mBio *6*, e01012.

Marcelino, T.P., Fala, A.M., da Silva, M.M., Souza-Melo, N., Malvezzi, A.M., Klippel, A.H., Zoltner, M., Padilla-Mejia, N., Kosto, S., Field, M.C.*, et al.* (2023). Identification of inhibitors for the transmembrane Trypanosoma cruzi eIF2alpha kinase relevant for parasite proliferation. J Biol Chem *299*, 104857.

Marek, M., Ramos-Morales, E., Picchi-Constante, G.F.A., Bayer, T., Norstrom, C., Herp, D., Sales-Junior, P.A., Guerra-Slompo, E.P., Hausmann, K., Chakrabarti, A.*, et al.* (2021). Species-selective targeting of pathogens revealed by the atypical structure and active site of Trypanosoma cruzi histone deacetylase DAC2. Cell Rep *37*, 110129.

Martel, D., Beneke, T., Gluenz, E., Spath, G.F., and Rachidi, N. (2017). Characterisation of Casein Kinase 1.1 in Leishmania donovani Using the CRISPR Cas9 Toolkit. Biomed Res Int *2017*, 4635605.

Melo, R.F.P., Guarneri, A.A., and Silber, A.M. (2020). The Influence of Environmental Cues on the Development of Trypanosoma cruzi in Triatominae Vector. Front Cell Infect Microbiol *10*, 27.

Minning, T.A., Weatherly, D.B., Atwood, J., 3rd, Orlando, R., and Tarleton, R.L. (2009). The steady-state transcriptome of the four major life-cycle stages of Trypanosoma cruzi. BMC Genomics *10*, 370.

Moreno, S.N., and Docampo, R. (2003). Calcium regulation in protozoan parasites. Curr Opin Microbiol *6*, 359-364.

Moreno, S.N., Silva, J., Vercesi, A.E., and Docampo, R. (1994). Cytosolic-free calcium elevation in Trypanosoma cruzi is required for cell invasion. J Exp Med *180*, 1535-1540.

Musheshe, N., Schmidt, M., and Zaccolo, M. (2018). cAMP: From Long-Range Second Messenger to Nanodomain Signalling. Trends Pharmacol Sci *39*, 209-222.

Nalefski, E.A., and Falke, J.J. (1996). The C2 domain calcium-binding motif: structural and functional diversity. Protein Sci *5*, 2375-2390.

Negreiros, R.S., Lander, N., Chiurillo, M.A., Vercesi, A.E., and Docampo, R. (2021). Mitochondrial Pyruvate Carrier Subunits Are Essential for Pyruvate-Driven Respiration, Infectivity, and Intracellular Replication of Trypanosoma cruzi. mBio *12*.

Oberholzer, M., Morand, S., Kunz, S., and Seebeck, T. (2006). A vector series for rapid PCR-mediated C-terminal in situ tagging of Trypanosoma brucei genes. Mol Biochem Parasitol *145*, 117-120.

Parsons, M., Worthey, E.A., Ward, P.N., and Mottram, J.C. (2005). Comparative analysis of the kinomes of three pathogenic trypanosomatids: Leishmania major, Trypanosoma brucei and Trypanosoma cruzi. BMC Genomics *6*, 127.

Peng, D., Kurup, S.P., Yao, P.Y., Minning, T.A., and Tarleton, R.L. (2014). CRISPR-Cas9-mediated single-gene and gene family disruption in Trypanosoma cruzi. mBio *6*, e02097-02014.

Peng, D., and Tarleton, R. (2015). EuPaGDT: a web tool tailored to design CRISPR guide RNAs for eukaryotic pathogens. Microb Genom *1*, e000033.

Rangel-Aldao, R., Triana, F., Fernandez, V., Comach, G., Abate, T., and Montoreano, R. (1988). Cyclic AMP as an inducer of the cell differentiation of Trypanosoma cruzi. Biochem Int *17*, 337-344.

Rohloff, P., Montalvetti, A., and Docampo, R. (2004). Acidocalcisomes and the contractile vacuole complex are involved in osmoregulation in Trypanosoma cruzi. J Biol Chem *279*, 52270-52281.

Rohloff, P., Rodrigues, C.O., and Docampo, R. (2003). Regulatory volume decrease in Trypanosoma cruzi involves amino acid efflux and changes in intracellular calcium. Mol Biochem Parasitol *126*, 219-230.

Saenz-Garcia, J.L., Borges, B.S., Souza-Melo, N., Machado, L.V., Miranda, J.S., Pacheco-Lugo, L.A., Moretti, N.S., Wheleer, R., Soares Medeiros, L.C., and DaRocha, W.D. (2021). Trypanin Disruption Affects the Motility and Infectivity of the Protozoan Trypanosoma cruzi. Front Cell Infect Microbiol *11*, 807236.

Schoijet, A.C., Miranda, K., Medeiros, L.C., de Souza, W., Flawia, M.M., Torres, H.N., Pignataro, O.P., Docampo, R., and Alonso, G.D. (2011). Defining the role of a FYVE domain in the localization and activity of a cAMP phosphodiesterase implicated in osmoregulation in Trypanosoma cruzi. Mol Microbiol *79*, 50-62.

Schoijet, A.C., Sternlieb, T., and Alonso, G.D. (2019). Signal Transduction Pathways as Therapeutic Target for Chagas Disease. Curr Med Chem *26*, 6572-6589.

Smircich, P., Eastman, G., Bispo, S., Duhagon, M.A., Guerra-Slompo, E.P., Garat, B., Goldenberg, S., Munroe, D.J., Dallagiovanna, B., Holetz, F.*, et al.* (2015). Ribosome profiling reveals translation control as a key mechanism generating differential gene expression in Trypanosoma cruzi. BMC Genomics *16*, 443.

Soares Medeiros, L.C., South, L., Peng, D., Bustamante, J.M., Wang, W., Bunkofske, M., Perumal, N., Sanchez-Valdez, F., and Tarleton, R.L. (2017). Rapid, Selection-Free, High-Efficiency Genome Editing in Protozoan Parasites Using CRISPR-Cas9 Ribonucleoproteins. mBio *8*.

Subota, I., Julkowska, D., Vincensini, L., Reeg, N., Buisson, J., Blisnick, T., Huet, D., Perrot, S., Santi-Rocca, J., Duchateau, M.*, et al.* (2014). Proteomic analysis of intact flagella of procyclic Trypanosoma brucei cells identifies novel flagellar proteins with unique sub-localization and dynamics. Mol Cell Proteomics *13*, 1769-1786.

Turra, G.L., Schneider, L., Liedgens, L., and Deponte, M. (2021). Testing the CRISPR-Cas9 and glmS ribozyme systems in Leishmania tarentolae. Mol Biochem Parasitol *241*, 111336.

Vazquez, M.P., and Levin, M.J. (1999). Functional analysis of the intergenic regions of TcP2beta gene loci allowed the construction of an improved Trypanosoma cruzi expression vector. Gene *239*, 217-225.

Velez-Ramirez, D.E., Shimogawa, M.M., Ray, S.S., Lopez, A., Rayatpisheh, S., Langousis, G., Gallagher-Jones, M., Dean, S., Wohlschlegel, J.A., and Hill, K.L. (2021). APEX2 Proximity Proteomics Resolves Flagellum Subdomains and Identifies Flagellum Tip-Specific Proteins in Trypanosoma brucei. mSphere *6*.

Wang, L., Wu, C., Peng, W., Zhou, Z., Zeng, J., Li, X., Yang, Y., Yu, S., Zou, Y., Huang, M.*, et al.* (2022). A high-performance genetically encoded fluorescent indicator for in vivo cAMP imaging. Nat Commun *13*, 5363.

WHO (2020). Chagas disease (American trypanosomiasis). Available online at: https://www.who.int/chagas/en/.

Won, M.M., Baublis, A., and Burleigh, B.A. (2023). Proximity-Dependent Biotinylation and Identification of Flagellar Proteins in Trypanosoma cruzi. mSphere *8*, e0008823.

Zhang, D., and Aravind, L. (2010). Identification of novel families and classification of the C2 domain superfamily elucidate the origin and evolution of membrane targeting activities in eukaryotes. Gene *469*, 18-30.

Legends of figures.

Figure 1. T7RNAP/Cas9 system for genome editing in *Trypanosoma cruzi*. A) Schematic representation of the general strategy used for CRISPR/Cas9-mediated gene deletion in *T. cruzi* cell line expressing T7RNAP and Cas9. This system requires constitutive expression of Cas9 and T7RNAP; sgRNA and donor DNAs are PCR-generated. The scheme shows the integration of the repair cassettes containing homologous regions (HR1 and HR2) after the double strand break generated by the ribonucleoprotein. sgRNA template including a T7 promoter is transfected along with donor DNAs. UTR, untranslated region; *PAC*, puromycin N-acetyltransferase; *BSD*, Blasticidin S deaminase. Horizontal black arrows indicate primers used for checking integration of donor DNA by PCR. **B)** Only one *TcAEK1* allele was disrupted at its genomic locus in the SKO cell lines. Lanes: M, 1-kb Plus ladder; C, T7RNAP/Cas9 control; SKO, *TcAEK1-SKO*; H_2O, PCR negative control. PCR fragment sizes: WT *TcAEK1*, 1,436 bp; *PAC*-replaced allele, 968 bp. **C)** Representative images displaying aberrant cell morphology and DNA content of a *TcAEK1-SKO* epimastigote. DIC, differential interference contrast. Merge image shows DAPI staining (blue) and DIC.

Figure 2. *TcCAMK* genome editing using a T7RNAP/Cas9 system. A) Schematic representation of the general strategy used for CRISPR/Cas9-mediated C-terminal endogenous tagging. *T. cruzi* epimastigotes constitutively expressing T7RNAP and Cas9 are transfected with two DNA fragments obtained by PCR: sgRNA template including a T7 promoter designed to target the 3' end of the gene of interest, and a donor DNA including homologous regions (HR1 and HR2) flanking a puromycin resistance cassette, to induce homologous direct repair. UTR, untranslated region; *Igr*, Tubulin intergenic region; *PAC*, puromycin N-acetyltransferase. Horizontal black arrows indicate primers used for checking integration of donor DNA by PCR. **B)** PCR verification of integration of donor DNA in the 3' end of the endogenous *TcCAMK* locus. *TcCAMK* allele sizes: WT, 240 bp; 3xc-Myc-tagged, 1,520 bp. Lanes: M, 1-kb Plus DNA ladder; C, T7RNAP/Cas9 control; CAMK-cMyc, *TcCAMK*-3xc-Myc; H_2O, PCR negative control. **C)** Western blot of *TcCAMK*-3xc-Myc (CAMK) using antibodies anti-c-Myc. Protein extract of the parental T7RNAP/Cas9 strain (T7/Cas9) was used as control. Tubulin was used as a loading control**. D)** Localization of endogenously tagged *TcCAMK*-3xc-Myc in epimastigotes using anti-

c-Myc antibodies. DIC, differential interference contrast. CAMK (green), *TcCAMK*-3xc-Myc. Merge 1 image shows *TcCAMK*-3xc-Myc (green) and DAPI staining (blue), and Merge 2 shows *TcCAMK*-3xc-Myc (green) and DIC. **E)** PCR verification of resistance cassette integration in both *TcCAMK* alleles. Lanes: M, 1-kb Plus DNA ladder; C, T7RNAP/Cas9 control; KO, *TcCAMK*-KO; H_2O, PCR negative control. PCR fragment sizes: WT *TcCAMK*, 1,960 bp; *PAC*-replaced allele, 1050 bp, *BSD* (Blasticidin S deaminase)-replaced allele, 850 bp. **F)** Growth of control (T7RNAP/Cas9) and *TcCAMK*-KO (CAMK-KO) epimastigotes in LIT medium ($n = 3$).

Figure 3. *TcFLAM6* genome editing using a T7RNAP/Cas9 system. A) PCR verification of integration of DNA donor in the 3' end of the endogenous *TcFLAM6* locus. *TcFLAM6* allele sizes: WT, 215 bp; 3xc-Myc-tagged, 1,476 bp. Lanes: M, 1-kb Plus DNA ladder; C, T7RNAP/Cas9 control; FLAM6-cMyc, *TcFLAM6*-3xc-Myc; H_2O, PCR negative control. **B)** Western blot of *TcFLAM6*-3xc-Myc (FLAM6) using antibodies anti-c-Myc. Protein extract of the parental T7RNAP/Cas9 (T7/Cas9) strain was used as control. Tubulin was used as a loading control**. C)** Localization of endogenously tagged *TcFLAM6*-3xc-Myc in epimastigotes using anti-c-Myc antibodies. DIC, differential interference contrast. FLAM6 (green), *TcFLAM6*-3xc-Myc. Merge 1 image shows *TcFLAM6*-3xc-Myc (green) and DAPI staining (blue), and Merge 2 shows *TcFLAM6*-3xc-Myc (green) and DIC. **D)** PCR verification of resistance cassette integration in *TcFLAM6* alleles. Lanes: M, 1-kb Plus DNA ladder; C, T7RNAP/Cas9 control; SKO, *TcFLAM6-SKO*; KO, *TcFLAM6-KO*; H_2O, PCR negative control. PCR fragment sizes: WT *TcFLAM6*, 4,252 bp; *PAC* (puromycin N-acetyltransferase)-replaced allele, 776 bp, *BSD* (Blasticidin S deaminase)-replaced allele, 576 bp. **E)** Growth of control (T7RNAP/Cas9) and *TcFLAM6*-KO (FLAM6-KO) epimastigotes in LIT medium. Values represent means ± SD of three independent replicates. (**$p < 0.01$, Student's t-test).

Figure 4. *TcCC2CP* genome editing using a T7RNAP/Cas9 system. A) PCR verification of integration of DNA donor in the 3' end of the endogenous *TcCC2CP* locus. *TcCC2CP* allele sizes: WT, 298 bp; 3xc-Myc-tagged, 1,578 bp. Lanes: M, 1-kb Plus DNA ladder; C, T7RNAP/Cas9 control; CC2CP-cMyc, *TcCC2CP*-3xc-Myc; H_2O, PCR negative control. **B)** Western blot of *TcCC2CP*-3xc-Myc (CC2CP) using antibodies anti-c-Myc. Protein extract of the parental T7RNAP/Cas9 strain was used as control. Tubulin was used as a loading control**. C)** Localization

of endogenously tagged *TcCC2CP*-3xc-Myc in epimastigotes using anti-c-Myc antibodies. DIC, differential interference contrast. CC2CP (green), *TcCC2CP*-3xc-Myc, Merge 1 image shows *TcCC2CP*-3xc-Myc (green) and DAPI staining (blue), and Merge 2 shows *TcCC2CP*-3xc-Myc (green) and DIC. **D)** Only one *TcCC2CP* allele was disrupted at its genomic locus in the SKO cell lines. Lanes: M, 1-kb Plus DNA ladder; C, T7RNAP/Cas9 control; SKO, *TcCC2CP*-SKO; H_2O, PCR negative control. PCR fragment sizes: WT *TcCC2CP*, 5,210 bp; *PAC* (puromycin N-acetyltransferase)-replaced allele, 745 bp. **E)** Growth of control (T7RNAP/Cas9) and *TcCC2CP-SKO* (CC2CP-SKO) epimastigotes in LIT medium. Student's t test was applied to growth rates calculated from each growth curve ($n = 3$; ***, $p < 0.001$, Student's t-test).

Table S1. Oligonucleotides used in this work.

N°	Primer name	Sequence (5′ → 3′)
1	RvG00	AAAAGCACCGACTCGGTGCCACTTTTTCAAGTTGATAACGGACTAGCCTTATTTTAACTTGCTATTTCTAGCTC TAAAAC
2	TcAEK1_sgRNA forward-KO	GAAATTAATACGACTCACTATAGG**AGTCTGGATGTACTTGGGAA**GTTTTAGAGCTAGAAATAGC
3	Fw_AEK1-KO	AAAAATTGTTTTTGAAGCTTTTCAAAAGGGACAAGAAGGAGCCGCGGGAATTCGATTATG
4	Rv_AEK1-KO	AAGACCTAATTTTTATTCAAGTGGTTATCCGCTGTGCCGCGAATTCACTAGTGATTTCAC
5	FwAEK1-KO check	ACACACACCGCAGTAAATATCTC
6	RvAEK1-KO check	TTTCTACCCTCGTCGTTCCC
7	TcCAMK_sgRNA forward_CTag	GAAATTAATACGACTCACTATAGG**TTCTAACACGAGGCGCCGCG**GTTTTAGAGCTAGAAATAGC
8	FwCAMK-CTag	CTTCCGCCCCTTTCTAACACGAGGCGCCGCGCCGGAAAGGGTACCGGGCCCCCCCTCGAG
9	RvCAMK-CTag	GAGAAAAAAAAAAAAAACAGGAGGCGTTTCTCGTTGGCGGCCGCTCTAGAACTAGTGGAT
10	FwCAMK-CTag check	TCGTGCCTCATTCACCGTTC
11	RvCAMK-CTag/KO check*	TCCTATTCTTGCTGACCTCC
12	TcCAMK_sgRNA forward_KO	GAAATTAATACGACTCACTATAGG**AGTCCAACTCTCGACTGCAG**GTTTTAGAGCTAGAAATAGC
13	FwCAMK-KO	AATTGGACTTCCAGGCACTACAGTCAACTTTGACGGAGGTGCCGCGGGAATTCGATTATG
14	RvCAMK-KO	CGCCTCGTGTTAGAAAGGGGCGGAAGTCGTGGCTCTGCGCGAATTCACTAGTGATTTCAC
15	FwCAMK-KO check	TTGAGAGGGCCTAGACAGAG
17	FLAM6 sgRNA forward cTag	GAAATTAATACGACTCACTATAGG**GCGCCCGTCGTGAGTGTTTG**GTTTTAGAGCTAGAAATAGC
18	FwFLAM6-CTag	GAGCGTGACGCCGTGTTTGCGGCTGCCAAGCGCCCGTCGGGTACCGGGCCCCCCCTCGAG
19	RvFLAM6-cTag	TTCATGCAAAAATAAACTTTGAGTTGCTCCACAATGGCGGCCGCTCTAGAACTAGTGGAT

20	FwFLAM6-CTag check	ATACCCTCCAAACCACTGCG
21	RvFLAM6-CTag check	TTTCTTCCCTACGCGCTCC
22	FLAM6 sgRNA forward_KO	GAAATTAATACGACTCACTATAGG**GGTGTGGGGAACCACTGCTG**GTTTTAGAGCTAGAAATAGC
23	FwFLAM6-KO	CATTGGCCACCGCGTCAATCGGTTCATCGTTCAGAAAGCGGCCGCGGGAATTCGATTATG
24	RvFLAM6-KO	CGCAAACACGGCGTCACGCTCCGCGACCCATCGCTCGCGCGAATTCACTAGTGATTTCAC
25	FwFLAM6-KO check	AACGAGTAGCTCATGCAGTC
26	RvFLAM6-KO check	TCCACAAACACTCACGACG
27	CC2CP sgRNA forward-CTag	GAAATTAATACGACTCACTATAGG**AGTACAGGGAGTGGATAGAA**GTTTTAGAGCTAGAAATAGC
28	CC2CP-CTag	GCCCTCGAAATGACACGCCCTTTGAGTACAGGGAGTGGAGGTACCGGGCCCCCCCTCGAG
29	CC2CP-CTag	CCGCAAGCTGGGCAACAGGGAAACGTGTGCCTTTTGGCGGCCGCTCTAGAACTAGTGGAT
30	FwCC2CP-CTag check	ATTACACAGACGTGGGTTCG
31	RvCC2CP-CTag/KO check*	AGTTGACCACACAAGTACACG
32	CC2CP sgRNA forward-KO	GAAATTAATACGACTCACTATAGG**GTGCGTGGGCTAATGATCGG**GTTTTAGAGCTAGAAATAGC
33	FwCC2CP-KO	CTTTTTATATTTACTTTTTTGCACCTTTCCGCGTGCCCATGCCGCGGGAATTCGATTATG
34	RvCC2CP-KO	CCGCCGCAAGCTGGGCAACAGGGAAACGTGTGCCTTTCGCGAATTCACTAGTGATTTCAC
35	FwCC2CP-KO Check	TGTGCCGTATACAACGTGT

Notes: *****reverse primers can be used in PCRs with the corresponding forward oligonucleotide to verify gene deletion or tagging. Bold: specific protospacer; underlined: gene-specific homologous region in primers used to amplify HDR DNA cassettes.

Figure 1.

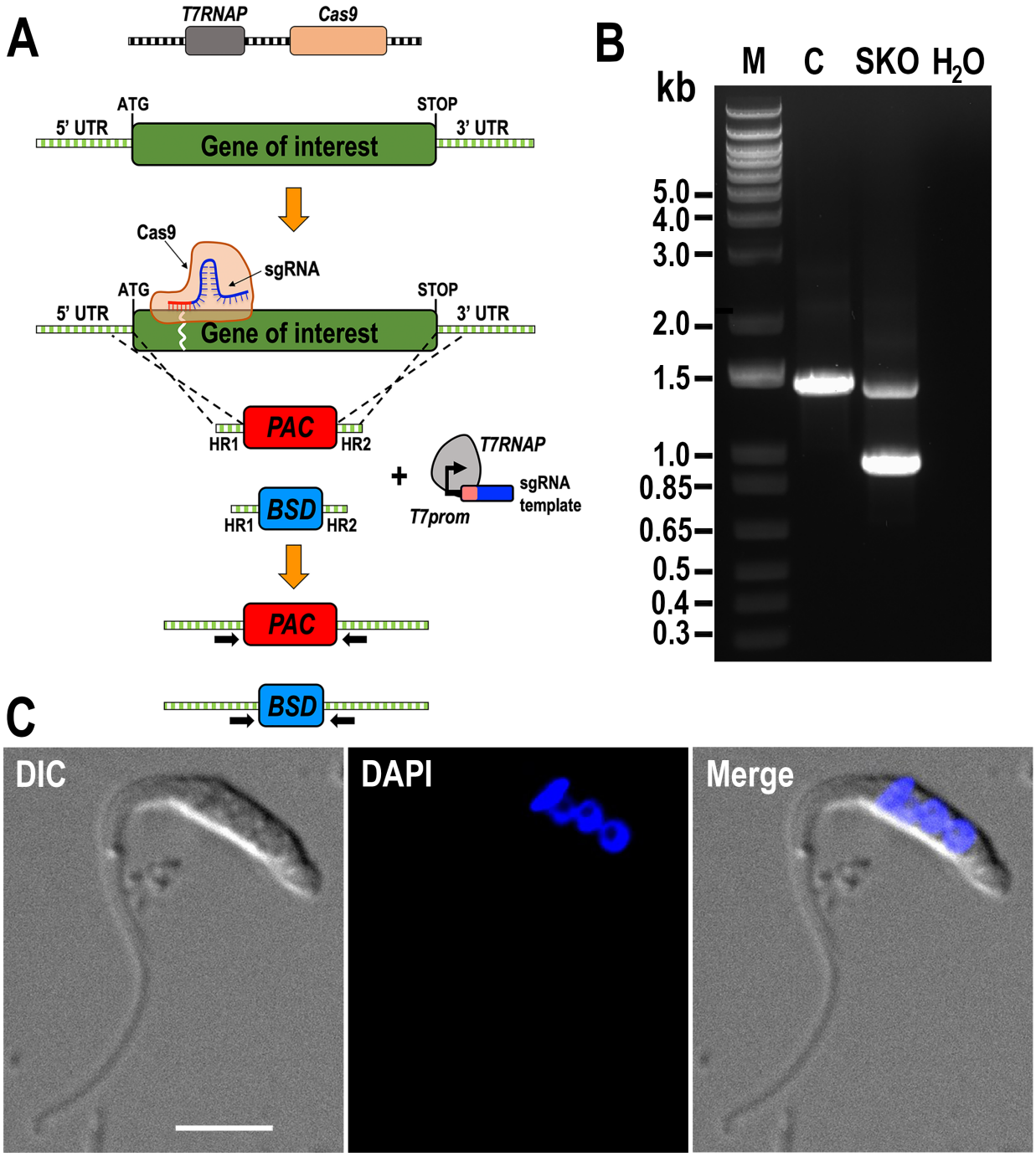
A
T7RNAP
Cas9
ATG
STOP
5' UTR
Gene of interest
3' UTR
Cas9
sgRNA
ATG
STOP
5' UTR
Gene of interest
3' UTR
PAC
HR1
HR2
T7RNAP
sgRNA
template
T7prom
BSD
HR1
HR2
PAC
BSD
B
kb
M
C
SKO
H2O
5.0
4.0
3.0
2.0
1.5
1.0
0.85
0.65
0.5
0.4
0.3
C
DIC
DAPI
Merge

Figure 2.

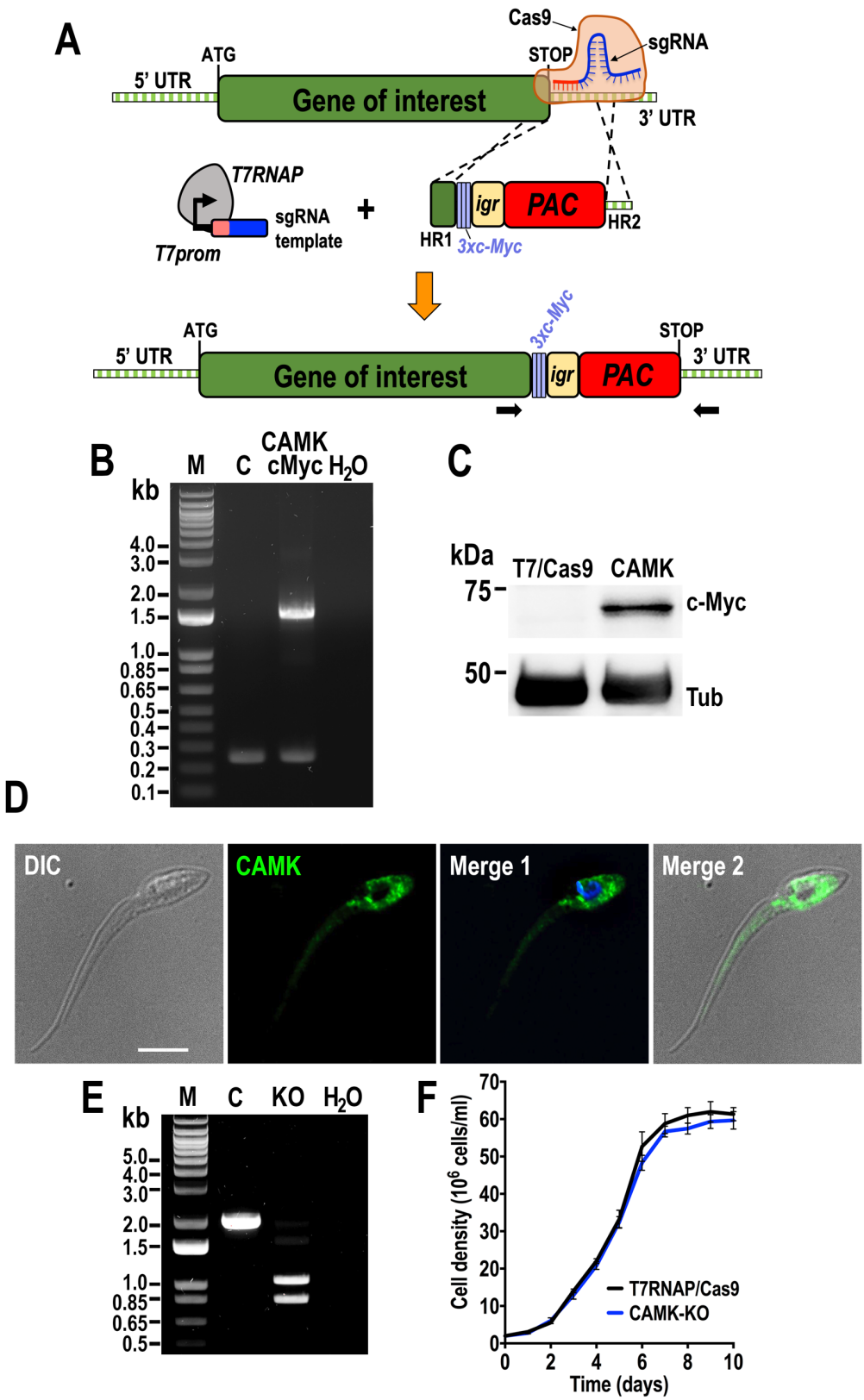
A
Cas9
sgRNA
ATG
STOP
5' UTR
Gene of interest
3' UTR
T7RNAP
sgRNA
template
T7prom
+
igr
PAC
HR1
3xc-Myc
HR2
ATG
3xc-Myc
STOP
5' UTR
Gene of interest
igr
PAC
3' UTR
B
M
C
CAMK
cMyc
H2O
kb
4.0
3.0
2.0
1.5
1.0
0.85
0.65
0.5
0.4
0.3
0.2
0.1
C
kDa
T7/Cas9
CAMK
75
c-Myc
50
Tub
D
DIC
CAMK
Merge 1
Merge 2
E
M
C
KO
H2O
kb
5.0
4.0
3.0
2.0
1.5
1.0
0.85
0.65
0.5
F
Cell density (10^6 cells/ml)
70
60
50
40
30
20
10
0
T7RNAP/Cas9
CAMK-KO
0
2
4
6
8
10
Time (days)

Figure 3.

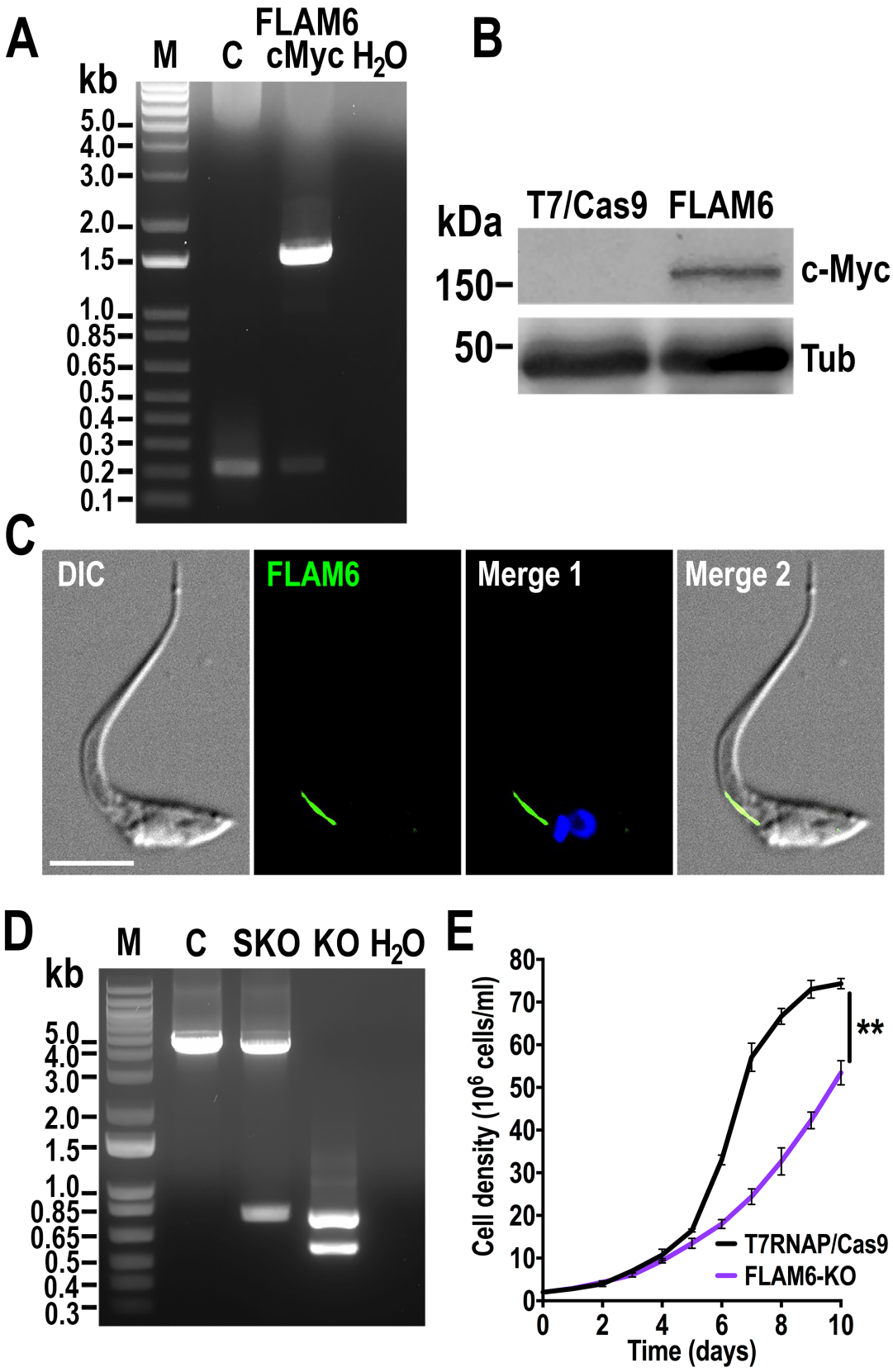
A
M
C
FLAM6
cMyc
H2O
kb
5.0
4.0
3.0
2.0
1.5
1.0
0.85
0.65
0.5
0.4
0.3
0.2
0.1
B
kDa
T7/Cas9
FLAM6
150
50
c-Myc
Tub
C
DIC
FLAM6
Merge 1
Merge 2
D
M
C
SKO
KO
H2O
kb
5.0
4.0
3.0
2.0
1.5
1.0
0.85
0.65
0.5
0.4
0.3
E
Cell density (10^6 cells/ml)
80
70
60
50
40
30
20
10
0
**
T7RNAP/Cas9
FLAM6-KO
0
2
4
6
8
10
Time (days)

Figure 4.

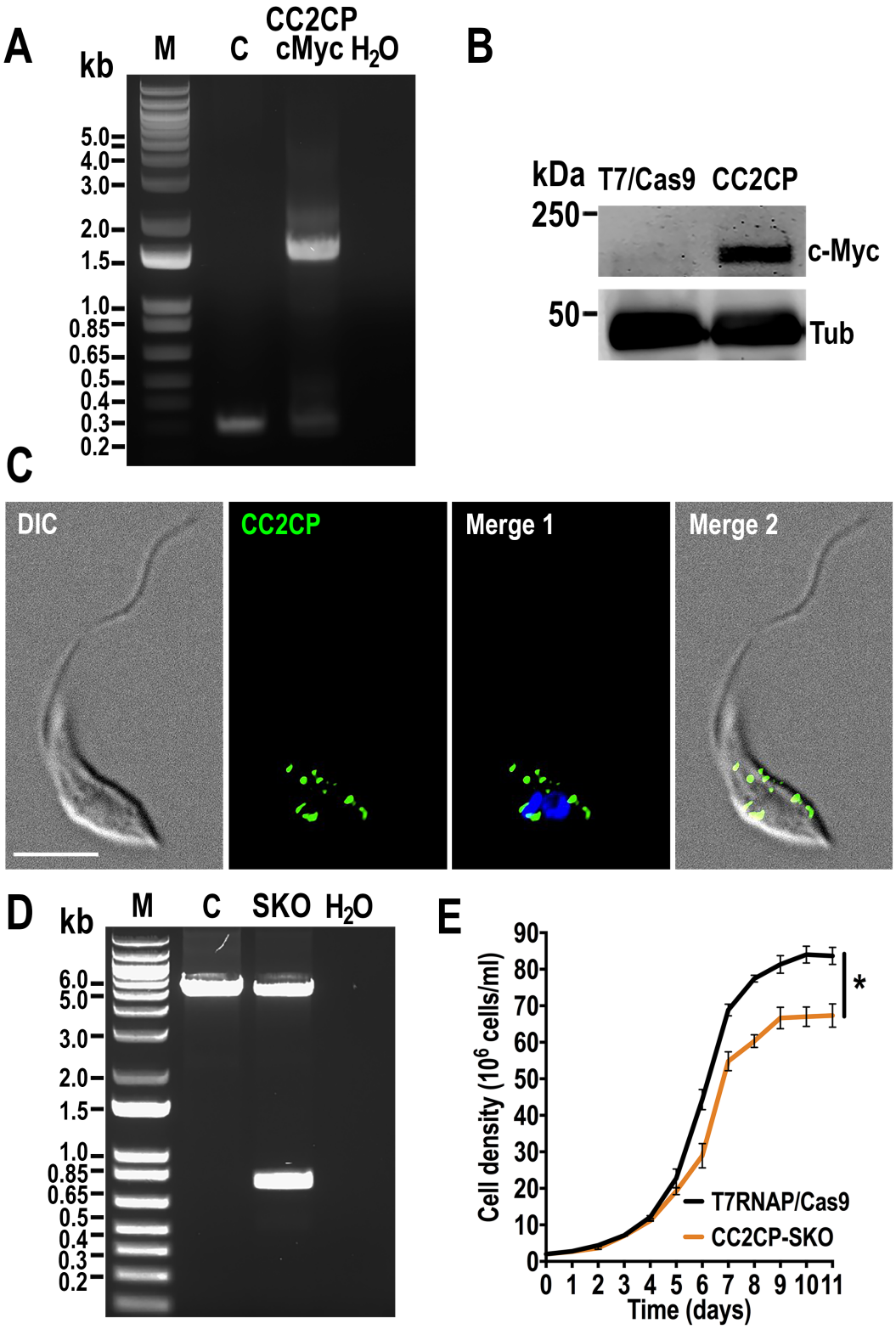
A
kb
M
C
CC2CP cMyc
H2O
5.0
4.0
3.0
2.0
1.5
1.0
0.85
0.65
0.5
0.4
0.3
0.2
B
kDa
T7/Cas9
CC2CP
250
c-Myc
50
Tub
C
DIC
CC2CP
Merge 1
Merge 2
D
kb
M
C
SKO
H2O
6.0
5.0
3.0
2.0
1.5
1.0
0.85
0.65
0.5
0.4
0.3
0.2
E
Cell density (10^6 cells/ml)
90
80
70
60
50
40
30
20
10
0
*
T7RNAP/Cas9
CC2CP-SKO
0 1 2 3 4 5 6 7 8 9 10 11
Time (days)